



## Impact of changing connecting rod and crankshaft on the performance and emissions of a diesel engine

Saeed Chamehsara 1, Mohammadreza Karami<sup>2\*</sup>

Young Researchers and Elite Club, Science and research branch, Islamic Azad University, Tehran, Iran

School of Mechanical Engineering, University of K.N. Toosi University of Technology, Tehran, Iran

### ARTICLE INFO

#### Article history:

Received : 27 Aug 2019

Accepted: 10 Oct 2019

Published: 1 Dec 2019

#### Keywords:

Diesel fuel engine

OM457

Compression ratio

Connecting rod

Crankshaft

Performance

Emissions

### ABSTRACT

Changing various parts of different types of engines in the maintenance phase was always a remarkable question. Purpose of the present study is identifying the performance and emissions of a diesel-fueled engine (OM457) before and after replacing connecting rod and crankshaft with another engine (OM444) in the same engine family.

At the first step, a solid model was made then some CFD analyses were done and, results were compared with previous studies for validation after that in the CFD modeling the impact of these parts replacement were observed, and the performance and emissions of this engine were compared with data before replacements.

As the result of these replacements, compression ratio and performance were decreased. HC and CO were increased due to lower air-fuel ratio, and NO<sub>x</sub> was decreased because of the lower temperature of in cylinder. Lowering the CR of a diesel engine will reduce the NO<sub>x</sub> emission numerously but the increase in other emissions will be slight. So for the environment issues lowering the CR will be a practical and low cost method.

## 1. Introduction

Nowadays According to the oil and environmental issues, lots of researches had been done to reduce the emissions and specific fuel consumption (SFC) of internal combustion engines (ICE). Among these issues improving the performance of an ICE is another concern. Therefore in this paper, the impact of different compression ratios (CR) on the emissions and performance of a heavy-duty diesel-fueled engine had been studied. The Otto and Diesel cycles are used to describe the processes happening in ICE. The thermodynamic analysis shows the effectiveness of both cycles to increase with growing compression ratio. Notably, the CR of spark-ignition engines usually are less than 10, while compression-ignition (CI) engines operate at CR above 15[1]. Heywood[2] unveiled impact of

CR on engine performance and thermal efficiency. Based on his study, mean effective pressure (MEP) were improved with growing CR until reaching a maximum value after that, MEP dropped with increasing the CR. According to Heisler's[3] study, improvement of MEP would cause peak cylinder pressure's increase.

Since the early 2000s using additives or even alternative fuels in ICE were noticed, therefore impact of CR on ICE performed by these fuels has been studied in many pieces of research. Cooney et al.[4] surveyed the ignition features of ethanol-gasoline mixtures, in an engine with constant load and constant speed with variable CR from 8:1 to 16:1. As a result of their study, CR is the primary factor in the early ignition stages. Based on Yücesu et al.[5]'s study, CR from 8:1 to 13:1 and fuel mixtures with ethanol content in gasoline up to

\*Corresponding Author

Email Address: [Mrk.mei77@gmail.com](mailto:Mrk.mei77@gmail.com)

<http://tlx.doi.org/10.22068/ijae.9.4.3130>

sixty percent, the output torque of their engine was increased by increasing the compression ratio. Costa et al.[6] experimentally studied the impact of CR on the performance of a spark-ignition engine which was fueled by two different fuels in various engine's speed. The results showed that higher CR would cause improvement on engine performance. Many other studies showed the improvement in the performance of an ICE by increasing the CR for different fuel additives [7]–[10].

Christensen et al.[11] studied the impact of different CR in a Homogeneous Charge Compression Ignition Engine (HCCI) as a result they mentioned the efficiency was not increased as much as expected by increasing CR. This was primarily because of a decrease in combustion efficiency with an increased CR. NOx emissions were very low (before and after the test.) and did not growth much with increased CR. Haraldsson et al.[12] studied the same case, and as a result they mentioned: Higher CR can be used as inlet air preheating. NOx emissions decrease, and brake thermal efficiency increases

The main reason of this study is to investigate the impact of decreasing CR of a diesel fuel engine on the performance and emission characteristics by modeling a heavy-duty engine in Converge CFD software .it is notable that the reduction in CR is because of using another engine's crankshaft and connecting rod and hadn't been chosen randomly.

## 2. Governing equations and case setup

Conservation of mass, momentum, and energy are the equations which govern the dynamics of fluid flow. The compressible equations for mass transport and momentum transport are given by:

$$\frac{\partial \rho}{\partial t} + \frac{\partial \rho u_i}{\partial x_i} = S \quad (1)$$

And

$$\frac{\partial \rho u_i}{\partial t} + \frac{\partial \rho u_i u_j}{\partial x_j} = -\frac{\partial P}{\partial x_i} + \frac{\partial \sigma_{ij}}{\partial x_j} + \rho g_i + S_i \quad (2)$$

Where the viscous stress tensor will be calculated by:

$$\sigma_{ij} = \mu \left( \frac{\partial u_i}{\partial x_j} + \frac{\partial u_j}{\partial x_i} \right) + \left( \mu' - \frac{2}{3} \mu \right) \frac{\partial u_k}{\partial x_k} \delta_{ij} \quad (3)$$

Where, In the above equations,  $\mu$  is viscosity,  $u$  is velocity,  $\rho$  is density,  $S$  is the source term,  $P$  represents pressure, and  $\delta_{ij}$  stands for the Kronecker delta.

The compressible form of the energy equation is given by:

$$\frac{\partial \rho e}{\partial t} + \frac{\partial u_j \rho e}{\partial x_j} = -P \frac{\partial u_j}{\partial x_j} + \sigma_{ij} \frac{\partial u_i}{\partial x_j} + \frac{\partial}{\partial x_j} \left( K \frac{\partial T}{\partial x_j} \right) + \frac{\partial}{\partial x_j} \left( \rho D \sum_m h_m \frac{\partial Y_m}{\partial x_j} \right) + S \quad (4)$$

Where, in the above equation  $\rho$  is density,  $h_m$  is the species enthalpy,  $P$  is the pressure,  $D$  is the mass diffusion coefficient,  $Y_m$  is the mass fraction of species  $m$ ,  $S$  is the source term,  $e$  is the specific internal energy,  $K$  is the conductivity,  $\sigma_{ij}$  is the stress tensor, and  $T$  is temperature.

### 2.1. Turbulence, spray and combustion models

In this paper for turbulence modeling RNG  $k - \varepsilon$  had been chosen. in this model turbulence kinetic energy (TKE) is the first additional equation. The second equation is turbulent dissipation ( $\varepsilon$ ), which is the difference between the standard and RNG  $k - \varepsilon$  turbulence models.

$$\frac{\partial \rho \varepsilon}{\partial t} + \frac{\partial (\rho u_i \varepsilon)}{\partial x_i} = \frac{\partial}{\partial x_j} \left( \frac{\mu}{Pr_\varepsilon} \frac{\partial \varepsilon}{\partial x_j} \right) + c_{\varepsilon 3} \rho \varepsilon \frac{\partial u_i}{\partial x_i} + \left( c_{\varepsilon 1} \frac{\partial u_i}{\partial x_j} \tau_{ij} - c_{\varepsilon 2} \rho \varepsilon + c_s S_s \right) \frac{\varepsilon}{k} - S + \rho R \quad (5)$$

Where in above question, the  $c_{\varepsilon i}$  terms are model constants that account for compression and expansion.  $S$  is the user-supplied source term, and  $S_s$  is the source term that represents the interactions with discrete phase (spray). Note that these two terms are distinct. Term  $R$  defines the difference between the standard and RNG  $k - \varepsilon$  models. In standard  $k - \varepsilon$  turbulence model, this term equals zero, and for the RNG model this term could be calculated by equation no.6.

$$R = \frac{c_\mu \eta^3 (1 - \eta/\eta_0) \varepsilon^2}{(1 + \beta \eta^3) k} \quad (6)$$

Where:

$$\eta = \frac{k}{\varepsilon} S_{ij} \quad (7)$$

And  $S_{ij}$  is the mean strain rate tensor[13].

In spray modeling for turbulent dispersion o'rouke model had been used[14]. For evaporation model, Frossling correlation had been used to determine the time rate of change of droplet size[15], and for the collision model, NTC Numerical Scheme had been used The NTC Numerical Scheme is based on those Schemes used in gas dynamics for Direct Simulation Monte Carlo (DSMC) calculations. This scheme had been proven to be much faster and more precise than the other schemes[16]. For combustion modeling, SAGE detailed chemistry solver had been used; SAGE calculates the reaction rates for each basic reaction, simultaneously the solver tries to solve the fundamental transport equations[17].

## 2.2. Geometry and initial condition

For CFD analysis a .stl file of piston head was required therefor by Solidworks software a solid model of OM457 Mercedes-Benz's piston head was developed shown in fig.1

After forming a suitable .stl file fluid volume must be extruded for CFD analyses. After that an

acceptable gridding strategy should be used, in the present study for reducing computational costs after using a base grid strategy AMR (adaptive mesh refinement) was used, by using this method

with high gradient in speed or pressure or temperature amount which was predetermined by user. Figure2 shows the fluid volume with gridding strategy in bottom dead center (BDC) and top dead center (TDC).

As it is so obvious in figure 2, where the fuel jets meet the edge of fluid volume, because of high gradient in thermodynamic parameters mesh cells automatically divide (darker areas in figure

For connecting rod's length and crank's radius which identifies the compression ratio of cylinder data of OM457 and OM444 were used according



Figure 1: OM457's piston head a: real one – b: .stl file of OM457's piston head used for CFD analyses

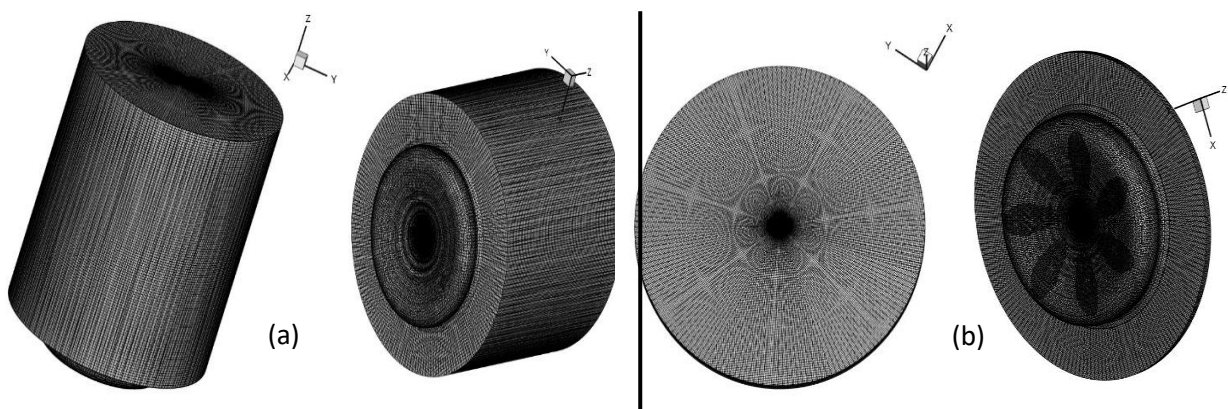


Figure 2: fluid volume with mesh cells a: in BDC – b: in TDC

mesh cells will divide automatically after facing

to data presented by Mercedes-Benz company as in table NO.1

**Table NO.1:** connecting rod's length and crank's radius of OM457 and OM444

| Engine | connecting rod's length | crank's radius |
|--------|-------------------------|----------------|
| OM457  | 250.906 mm              | 77.36 mm       |
| OM444  | 256.21 mm               | 70.802 mm      |

For initial values, the same values were used as in Afshari et al. [18] 's work which are presented in table No.2

**Table No.2:** initial values of the case study

|                               |                     |
|-------------------------------|---------------------|
| Intake valve close            | -144 crank angel    |
| Exhaust valve open            | 116 crank angel     |
| Intake valve open             | 336 crank angel     |
| Exhaust valve close           | 387 crank angel     |
| injection start               | -13.727 crank angel |
| injection end                 | 20.92 crank angel   |
| Mass of fuel                  | 0.152 gr/cycle      |
| Maximum of injection pressure | 1795 bar            |
| Bore                          | 128 mm              |

According to the technical data of OM457, presented by Mercedes-Benz the rated power of this engine at an engine speed of 2000 rpm would be 260 kW and mean effective pressure would be 13.03 bar at this engine speed.

### 3. Validation

For validation torque and specific NO<sub>x</sub> of OM457 modeled in the present study were

measured in various engine speeds and compared with those in Afshari et al. [18]'s study as in Figure 3 and 4. This two parameters were chosen as the symbol of their categories. Torque was chosen showing the correctness of performance estimation and NO<sub>x</sub> for emissions estimation.

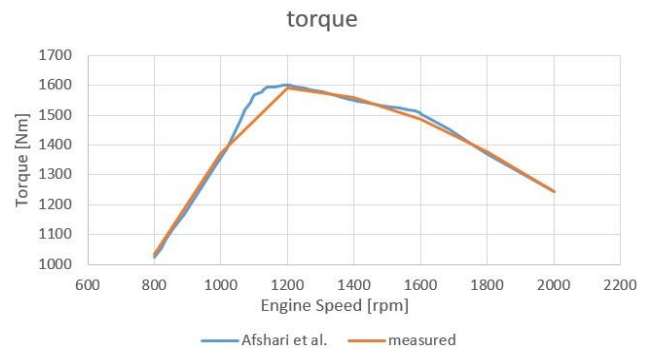


**Figure 3:** torque comparison of Afshari et al.[18]'s study with present study for OM457

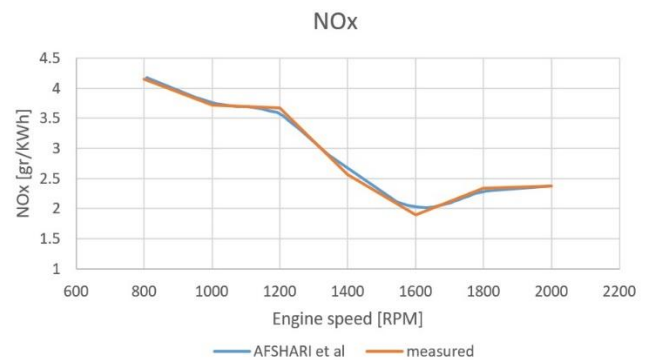


**Figure 4:** NO<sub>x</sub> comparison of Afshari et al.[18]'s study with present study for OM457

As it is clear the present study's modeling of the OM457 diesel engine is in an acceptable accommodation with Afshari et al.[18]'s study (errors were less than 5%). As the result, the present study's approach and models are validated. It's noticeable that torque and NO<sub>x</sub>'s value were measured just for engine speeds of 800-1000-1200-1400-1600-1800-2000 (rpm) and they weren't measured continuously as the result we didn't expect accommodation in engine speeds among these engine speeds.

#### 4. Result and discussion

At the first step compression ratio of the cylinder should be calculated before CFD analysis. CR of OM457 original engine is 18.5 ( based on data presented by Mercedes-Benz) after replacement of connecting rod and crankshaft of OM444 with the ones of OM457 the CR of new engine will be 14.52 , now after calculating the new CR, two different cases were set up with same initial conditions of table no.2 and different CR according to table no.1 and same piston head geometry to evaluate the performance and emissions of a diesel engine after replacement of connecting rod and crankshaft of another engine.

Now after setting up these cases, CFD analyses were done with Converge CFD software. As the result of these analyses for OM457 results were shown in table no.3

**Table no.3:** results of OM457

|                  |           |
|------------------|-----------|
| Duration (deg)   | 260.045   |
| Gross work (J)   | 2685.52   |
| IMEP (Pa)        | 1.304e+06 |
| Net work (J)     | 2597.03   |
| HRR peak (J/deg) | 212.718   |

As in table no.3, IMEP is in good accommodation with data presented by Mercedes-Benz (13.03 bar from technical data from the company and 13.04 bar from Converge CFD software output.)

Power and torque of engine will be calculated based on Heywood [2]’s formula as below:

$$P_i(W) = \frac{W_{c,i}(J)N^{(rev/S)}}{n_R} \quad (8)$$

$$P(kW) = 2\pi N^{(rev/S)}T(N.m) * 10^{-3} \quad (9)$$

Where  $P_i$  is indicator power.  $W_{c,i}$  is net work. N is engine speed, and  $n_R$  is 2 for a four-stroke engine, finally, T is output torque of the engine.

N=2000 (rpm) so it is equal to 33.33 (rev/s) and after using net work from table no.3 power and torque of each cylinder would be:

$$P_i(W) = \frac{2597.03 * 33.333}{2} = 43283.8W$$

$$P_i(kW) = 43.283 KW$$

$$T(N.m) = \frac{43.283 * 10^3}{2\pi * 33.33} = 206.67(N.m)$$

So for a six cylinder engine’s (main OM457 engine) torque and power in engine speed of 2000 (rpm) would be:

$$P_i(kW) = 259.698$$

$$T(N.m) = 1240.015$$

The same approach was used for the new engine (OM457 with connecting rod and crankshaft of OM444), table no.4 is the results of CFD analyses for this engine.

**Table no.4:** results of the new engine

|                  |            |
|------------------|------------|
| Duration (deg)   | 260.016    |
| Gross work (J)   | 2321.91    |
| IMEP (Pa)        | 1.2284e+06 |
| Net work (J)     | 2238.41    |
| HRR peak (J/deg) | 191.605    |

According to equations number (8) and (9) power and torque of this engine’s cylinder would be:

$$P_i(kW) = 37.303$$

$$T(N.m) = 178.115$$

So for a six cylinder engine with this characteristics power and torque would be:

$$P_i(kW) = 223.818$$

$$T(N.m) = 1068.69$$

In figure number 5 in-cylinder pressure – crank’s angel (P-  $\theta$ ) for these two engines had been graphed.

After comparing the performance of these two engines now, it is time to compare their emissions.

For this purpose in figures number 6 – 8 emissions of NO<sub>x</sub> – HC and CO for these two engines are presented.

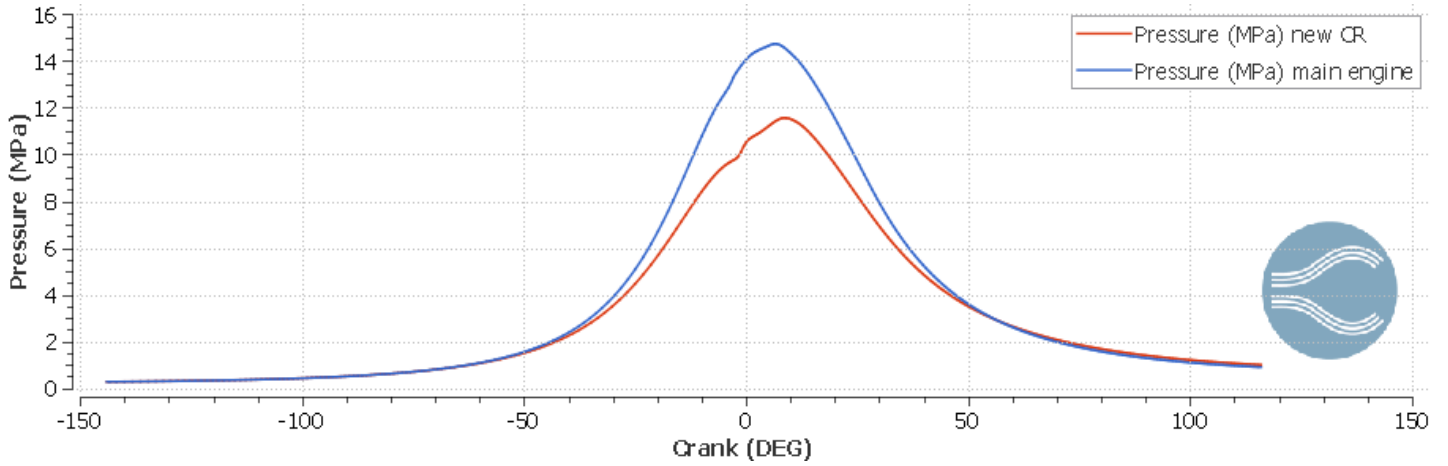


**Figure 5:** P-  $\theta$  for OM457 and the new engine with lower CR

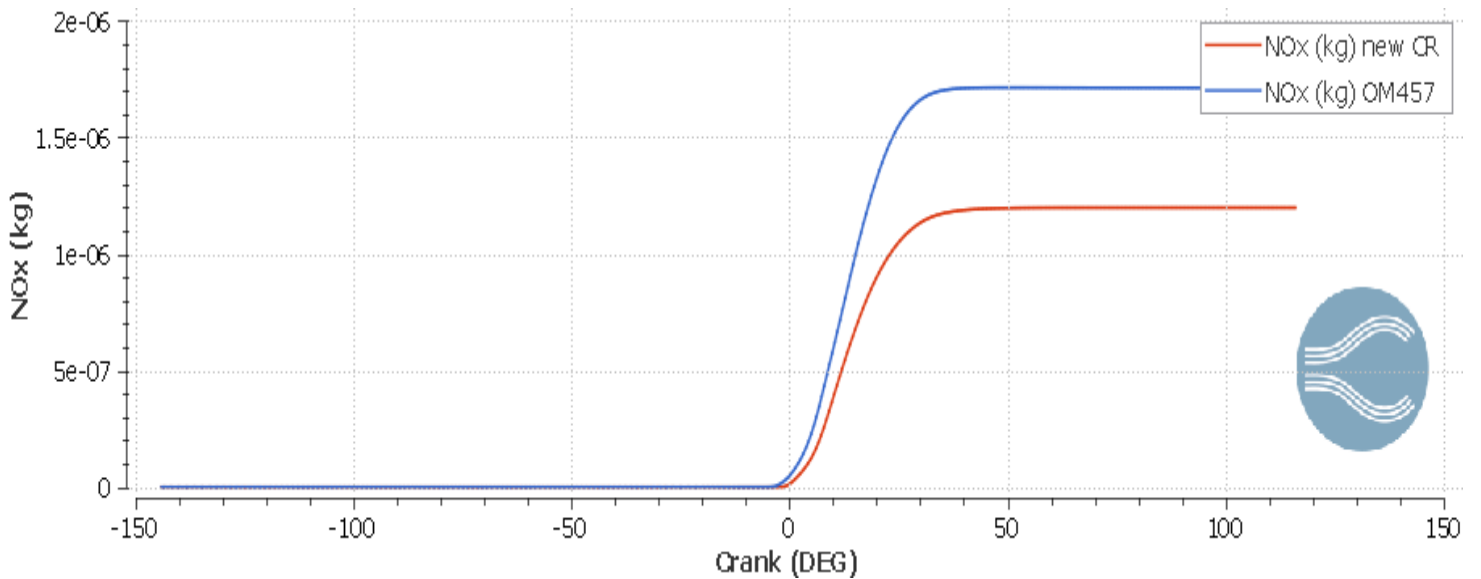


**Figure 6:** comparison of NO<sub>x</sub> emission for OM457 original and new engine with replacements



## Impact of changing connecting rod and crankshaft on the performance and emissions of a diesel engine

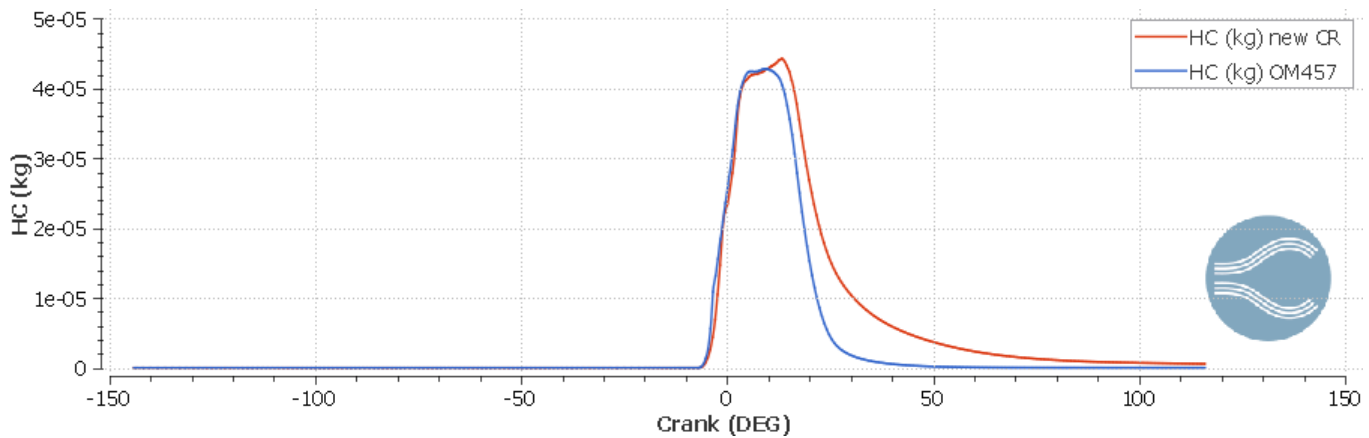


Figure 7: comparison of HC emission for OM457 original and new engine with replacements

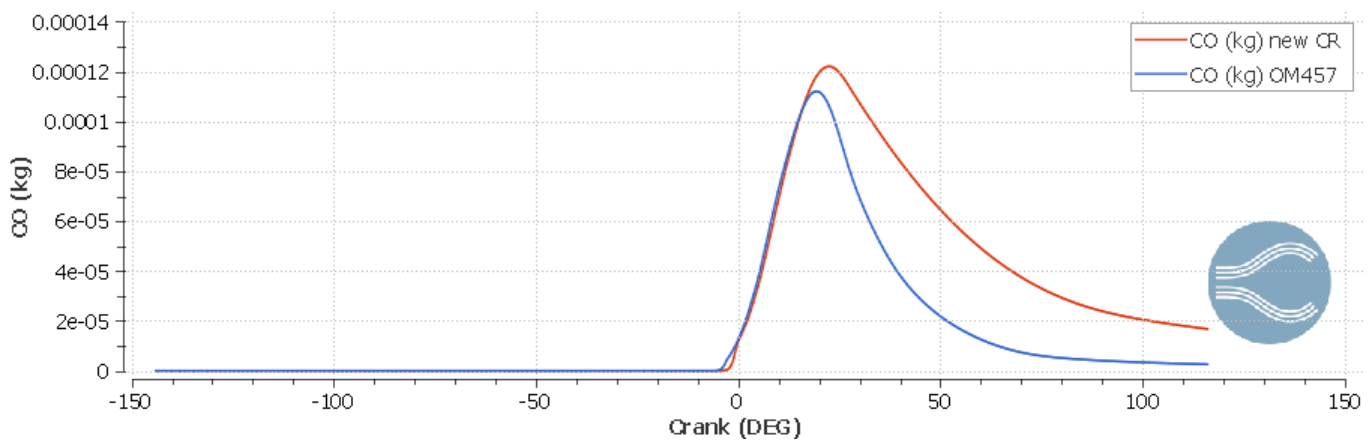


Figure 8: comparison of CO emission for OM457 original and new engine with replacements

### 5. Conclusions

In the present study at the first step piston head of OM457 diesel fuel engine was modeled, then this engine was studied. Results of CFD modeling in this study were validated with other studies for this engine. After that connecting rod and crankshaft of this engine was replaced with the ones of the OM444 diesel engine as the result compression ratio of the engine was changed. After this replacement, these two engines were studied, and their performance and emissions were compared due to some CFD analyses by CONVERGE CFD software.

From this study following observation regarding comparing the data among these segments were recorded:

- By replacing the connecting rod and crankshaft of OM444 with the ones of OM457 the compression ratio will decrease from 18.5 to 14.52
- In the new engine set up, the reduction of 13.8% in output torque and power had been observed.
- Reduction in  $\text{NO}_x$  emission was observed after replacement of connecting rod and crankshaft. This reduction is mainly because of reduction of in-cylinder temperature.
- Increase in unburned hydrocarbons and carbon monoxide were observed due to the reduction of air-fuel ratio.

- As the result by changing the crankshaft and connecting rod NO<sub>x</sub> emission was reduced by 33% therefor according to the environmental issues lowering the CR will help. For reducing other emissions using EGR and changing fuel spray's characteristics will be helpful.

## References

- [1] S. A. Klein, "An Explanation for Observed Compression Ratios in Internal Combustion Engines," *J. Eng. Gas Turbines Power*, vol. 113, no. 4, p. 511, Oct. 1991.
- [2] J. B. Heywood, *Internal combustion engine fundamentals*. McGraw-Hill, 1988.
- [3] H. Heisler, "Advanced Engine Technology Hodder Headline Group," 1995.
- [4] C. P. Cooney, Yeliana, J. J. Worm, and J. D. Naber, "Combustion Characterization in an Internal Combustion Engine with Ethanol-Gasoline Blended Fuels Varying Compression Ratios and Ignition Timing," *Energy & Fuels*, vol. 23, no. 5, pp. 2319–2324, May 2009.
- [5] H. S. Yücesu, T. Topgül, C. Çinar, and M. Okur, "Effect of ethanol-gasoline blends on engine performance and exhaust emissions in different compression ratios," *Appl. Therm. Eng.*, vol. 26, no. 17–18, pp. 2272–2278, Dec. 2006.
- [6] R. C. Costa and J. R. Sodré, "Compression ratio effects on an ethanol/gasoline fuelled engine performance," *Appl. Therm. Eng.*, vol. 31, no. 2–3, pp. 278–283, Feb. 2011.
- [7] M. EL\_Kassaby and M. A. Nemit\_allah, "Studying the effect of compression ratio on an engine fueled with waste oil produced biodiesel/diesel fuel," *Alexandria Eng. J.*, vol. 52, no. 1, pp. 1–11, Mar. 2013.
- [8] H. Raheman and S. V. Ghadge, "Performance of diesel engine with biodiesel at varying compression ratio and ignition timing," *Fuel*, vol. 87, no. 12, pp. 2659–2666, Sep. 2008.
- [9] "Experimental investigation of the effect of compression ratio and injection pressure in a direct injection diesel engine running on Jatropa methyl ester," *Appl. Therm. Eng.*, vol. 30, no. 5, pp. 442–448, Apr. 2010.
- [10] K. Muralidharan and D. Vasudevan, "Performance, emission and combustion characteristics of a variable compression ratio engine using methyl esters of waste cooking oil and diesel blends," *Appl. Energy*, vol. 88, no. 11, pp. 3959–3968, Nov. 2011.
- [11] M. Christensen, A. Hultqvist, and B. Johansson, "Demonstrating the Multi Fuel Capability of a Homogeneous Charge Compression Ignition Engine with Variable Compression Ratio," 1999.
- [12] G. Haraldsson, P. Tunestål, B. Johansson, and J. Hyvönen, "HCCI Combustion Phasing in a Multi Cylinder Engine Using Variable Compression Ratio," *SAE Transactions*, vol. 111. SAE International, pp. 2654–2663, 2002.
- [13] Amirhasan Kakaee and Mohammadreza Karami, "Comparison of different turbulence models in a high-pressure fuel jet," *Int. J. Automot. Eng.*, vol. 9, no. 2, pp. 2949–2957, 2019.
- [14] P. J. O'Rourke and A. A. Amsden, "A Spray/Wall Interaction Submodel for the KIVA-3 Wall Film Model," *SAE Transactions*, vol. 109. SAE International, pp. 281–298, 2000.
- [15] A. A. Amsden, P. J. O'Rourke, and T. D. Butler, "KIVA-2: A computer program for chemically reactive flows with sprays," *Unknown*, vol. 89, 1989.
- [16] D. P. Schmidt and C. J. Rutland, "A New Droplet Collision Algorithm," *J. Comput. Phys.*, vol. 164, no. 1, pp. 62–80, Oct. 2000.
- [17] C. CFD, *CONVERGE-2.3- MANUAL*. .
- [18] D. Afshari, A. Afrabandpey, and R. Aghamohammadi, "Deploying Variable Valve Timing System in 'OM457' Diesel Engine to Reduce Specific Fuel Consumption and Its Impact on Emissions," *researchgate.net*.